Alpha 6 Integrins Regulate the Expression of Laminin-511 and CXCR4 to Promote Endothelial Tubular Morphogenesis

Hao Xu, Kevin Pumiglia and Susan E. LaFlamme*

Department of Regenerative and Cancer Cell Biology
Albany Medical College
Albany NY 12208

Running Title: Endothelial morphogenesis

Corresponding author: laflams@amc.edu

Key words: Integrin, laminin, CXCR4, angiogenesis

21 **Summary statement**

22

23 Endothelial-secreted laminin-511 and its receptors, α6 integrins promote tubular morphogenesis
24 by regulating the expression of the chemokine receptor, CXCR4. Additionally, the depletion of
25 α6 integrins from established tubes results in the loss of tubular integrity and laminin-511
26 expression.

27

28

Abstract (180 words)

During angiogenesis, endothelial cells engage components of the extracellular matrix through integrin-mediated adhesion. Endothelial cells express laminin-411 and laminin-511 that bind to integrins, including the α6 integrins, α6β1 and α6β4. However, little is known about the contribution of these laminins to endothelial tubular morphogenesis and stability. We used two organotypic angiogenesis assays in conjunction with RNAi approaches to demonstrate that endothelial depletion of either the α4 chain of laminin-411 or the α5 chain of laminin-511 inhibited sprouting and tube formation. Depletion of α6 integrins resulted in similar phenotypes. Interestingly, depletion of α6 integrins also inhibited the expression of laminin-511, which correlated with the loss of tubular stability. Loss of either α6 integrins or laminin-511 resulted in the inhibition of the expression of CXCR4, a gene previously associated with sprouting endothelial cells. Pharmacological inhibition of CXCR4 signaling suppressed endothelial sprouting and morphogenesis, suggesting that α6 integrins and laminin-511 promotes endothelial tubular morphogenesis in part by regulating the expression of CXCR4. Taken together, our results suggest that α6 integrins regulate gene expression to promote both early events in tubular morphogenesis, as well as the stability of established endothelial tubes.

Introduction

Angiogenesis is a process by which new vessels sprout from pre-existing vasculature, anastomose with neighboring sprouts to form new networks, which then remodel and mature (Carmeliet, 2003). Angiogenesis contributes to both normal and pathological processes, including tissue repair, tumor progression, and inflammation (Carmeliet, 2005). Thus, understanding the mechanisms that regulate various aspects of this process remains an important objective.

Endothelial cells interact with components of the extracellular matrix (ECM), including fibronectin, to promote early stages of angiogenesis, whereas the binding of endothelial cells to components of the basement membrane, such as laminin, contributes to vessel stability (Song et al., 2017; Thyboll et al., 2002). Although endothelial cells can adhere to ECM components provided by other cell types, such as those present in the provisional matrix that is formed during tissue repair (Eming et al., 2007), endothelial cells themselves secrete both ECM and basement membrane components, including fibronectin and laminins (Hallmann et al., 2005; Turner et al., 2017).

Laminins are heterotrimeric proteins, containing α, β and γ chains (Yurchenco, 2011). Endothelial cells express laminin-411, which contains the α4, β1 and γ1 chains and laminin-511, which contains the α5, β1 and γ1 chains (Hallmann et al., 2005). Current data suggests that these laminins support vessel stability. The global deletion of the laminin-α4 (Lm- α4) chain resulted in embryonic hemorrhaging (Thyboll et al., 2002), whereas the endothelial-specific deletion of Lm- α5 chain reduced endothelial barrier function (Song et al., 2017). Both of these phenotypes suggest that these laminin isoforms promote vessel stability; however, whether these laminins are required for endothelial tubular morphogenesis has not been examined.

Integrins are α/β heterodimeric receptors that bind to ECM proteins and components of the basement membrane, including laminins, to mediate adhesion and to activate signaling pathways that cooperate with growth factor receptors to regulate cell behavior (Danen and Sonnenberg, 2003; Streuli and Akhtar, 2009). Endothelial cells express several integrin heterodimers that allow their interaction with components of the extracellular matrix including fibronectin and collagen, as well as laminins present in the endothelial basement membrane (Avraamides et al., 2008; Davis and Senger, 2005). Our current study focuses on determining whether laminin-411 and laminin-511 and their integrin receptors, α6 integrins (α6β1 and α6β4) contribute to early steps in endothelial tubular morphogenesis (Hallmann et al., 2005; Kortesmaa et al., 2000).

Other labs have previously analyzed the role of α6 integrins in angiogenesis. Mice with the Tie 1-dependent endothelial deletion of the α6 integrin subunit showed that the depletion of α6 integrins promoted angiogenesis (Germain et al., 2010), presumably due in part to the reduced association of endothelial cells with their underlying basement membrane. Interestingly, the Tie 2-dependent endothelial deletion of α6 integrins resulted in reduced angiogenesis; this was explained by the loss of α6 integrins on endothelial progenitor cells and Tie-2 expressing macrophages (Bouvard et al., 2010; Bouvard et al., 2014). Notably, *in vitro* and explant angiogenesis assays demonstrated a requirement for α6 integrins; however, this requirement was dependent upon the ECM microenvironment (Bouvard et al., 2010; Bouvard et al., 2014; Lee et al., 2006; Primo et al., 2010; Samarelli et al., 2014).

The onset of angiogenesis requires the disruption of stable interactions of endothelial cells with their basement membrane. Thus, to isolate the contribution of laminins and their integrin receptors to early steps in endothelial tubular morphogenesis, we used two organotypic co-culture models that do not require the destabilization of existing tubes. We asked whether the endothelial expression of laminin-411 and/or laminin-511 is required for endothelial tubular morphogenesis, and if so, whether α6 integrins were also required. Our data demonstrate that depleting endothelial cells of the LM-α4 chain, the LM-α5 chain, or the integrin α6 subunit inhibits endothelial morphogenesis. This is the first report demonstrating that endothelial-secreted laminins can contribute to this process. Additionally we show that the expression of laminin-511 and α6 integrins regulate the expression of the proangiogenic gene CXCR4 (Salcedo and Oppenheim, 2003; Salvucci et al., 2002; Tachibana et al., 1998; Unoki et al., 2010). Furthermore, the pharmacological inhibition of CXCR4 impairs tubulogenesis demonstrating that the regulation of CXCR4 by α6 integrins and laminin-511 contributes to tubular morphogenesis. Lastly, we show that α6 integrins regulate the stability of endothelial tubes at least in part by regulating the expression of the α5 chain of laminin-511. Taken together, our data suggests that the interaction of α6 integrins and laminin-511 contributes to angiogenesis by regulating the expression of CXCR4 in early stages of endothelial morphogenesis, and that once tubes have formed the interaction of α6 integrins and laminin-511 promotes the stability of endothelial tubes.

113 **Results**

114

115 **Endothelial laminins regulate endothelial tubulogenesis**

116 To examine the contribution of endothelial laminin-411 and laminin-511 in tubular
117 morphogenesis, we employed RNAi technology in conjunction with two organotypic
118 angiogenesis assays: the planar co-culture model and the bead sprout assay. In the planar co-
119 culture model, human endothelial cells (HUVECs) are plated at very low density on a confluent
120 layer of human dermal fibroblasts (Bishop et al., 1999). Endothelial cells then proliferate and
121 migrate to form cell trains/cords, which then form lumenized tubes over time (Bishop et al.,
122 1999; Mavria et al., 2006). In the bead sprout assay, endothelial cells are adhered to cytodex
123 beads and embedded in a fibrin gel, which is then covered with a confluent layer of human
124 dermal fibroblasts. Endothelial cells sprout out from the beads into the fibril gel and form
125 lumenized tubes over time (Nakatsu and Hughes, 2008; Nakatsu et al., 2003). Importantly,
126 endothelial cells express laminin-411 and laminin-511 in addition to Col IV in both organotypic
127 models as demonstrated by immunofluorescence microscopy (Fig. 1A-B)

128 To determine whether the expression of either laminin-411 or laminin-511 was necessary
129 for endothelial morphogenesis, we inhibited their expression with siRNA targeting either the α4
130 chain of laminin-411 or the α5 chain of laminin-511. Data was analyzed from three independent
131 experiments. The efficiency of knockdown in each experiment was determined by qPCR (Fig.
132 1C-D). Interestingly, knockdown of either LM-α5 or α4 chains caused defective endothelial
133 morphogenesis in planar co-culture with a more dramatic phenotype resulting from inhibiting the
134 expression of the α5 chain (Fig. 1E-F). Quantitation of the lengths of cell trains/cords formed
135 after two days showed a mean length of 340 μm in control, whereas depletion of either the Lm-
136 α4 or-α5 chain resulted in an average length of 175 μm and 95 μm, respectively. Similarly,
137 depletion of either laminin chain inhibited sprouting in the bead-sprout assay (Fig. 1G-I). Both
138 the number and lengths of sprouts were decreased (Fig. 1H-I). Our data indicate that both
139 laminin-411 and laminin-511 contribute to endothelial sprouting and tube formation and that the
140 expression of one isoform cannot compensate for the loss of the other suggesting that each
141 laminin isoform may play distinct role during tubular morphogenesis.

142

143 **Endothelial α6 integrins promote tubular morphogenesis**

144 Since α6 integrins have been shown to bind to both laminin-411 and laminin-511 (Kortesmaa et
145 al., 2000), we were interested to test the requirement for α6 integrins in our organotypic models
146 and to determine whether depletion of α6 integrins phenocopied the loss of laminin-411 or

147 laminin-511. As expected, endothelial cells express α6 integrins in co-culture (Fig. 2A). To
148 determine the effect of depleting endothelial cells of α6 integrins, we employed lentiviral vectors
149 for the doxycycline inducible expression of a non-targeting shRNA or shRNAs targeting the
150 integrin α6 subunit. Induction of these shRNAs results in the co-expression of a GFP reporter.
151 Endothelial cells were transduced with these lentiviral vectors and the expression of shRNAs
152 was induced by the addition of doxycycline. Effects of α6 depletion on endothelial
153 morphogenesis in the planar co-culture were analyzed in three independent experiments. The
154 efficiency of knockdown from these experiments was analyzed by western blot (Fig. 2B, left
155 panel). Effects on endothelial cord/tube length were quantified every two days for a total of 10
156 days (Fig. 2B, middle panel). Images of representative co-cultures at day 6 are shown in Figure
157 2B (right panel). Taken together, the data show that morphogenesis is inhibited by day 2 and
158 remained suppressed with very little lengthening of individual endothelial cords in the α6-
159 depleted condition at day 10. Similar results were obtained with two additional shRNA targeting
160 sequences (Supplemental Fig. 1).
161 The depletion of α6 integrins had a similar inhibitory effect in the bead sprout assay (Fig.
162 2C). Data was obtained from three independent experiments in which α6 expression was
163 inhibited by the induction of α6 targeting shRNA (Fig. 2C, left panel). Measurements of sprout
164 length overtime revealed that endothelial sprouting remained inhibited throughout the 8-day
165 assay (Fig. 2C, middle panel). Images of representative bead sprouts formed at day 8 by control
166 and α6 depleted endothelial cells are shown in Fig. 2C (right panel). The depletion of α6
167 integrins phenocopies the depletion of the LM-α5 chain and LM-α4 chain, suggesting that the
168 interaction between α6 integrins and laminins secreted by endothelial cells is crucial for tubular
169 morphogenesis.
170

171 **The expression of α6 integrins promotes endothelial tube integrity**

172 Given our results that α6 integrins are required for tubulogenesis in our organotypic assays,
173 we asked whether these integrins are also required for the stability of established tubes. To
174 accomplish this, planar co-cultures were set up with endothelial cells that were transduced with
175 lentiviruses carrying either α6-targeting or non-targeting shRNAs. Co-cultures were incubated in
176 the absence of doxycycline for 10 days at which time normal endothelial tubes were well
177 established. Co-cultures were then treated with doxycycline to induce the expression of non-
178 targeting or α6-targeting shRNAs and imaged after 8 and 12 days of doxycycline treatment.
179 Endothelial tubes expressing α6 shRNA progressively became destabilized over time (Fig. 3A),
180 which was quantified as changes in the morphology of endothelial structures (Fig. 3B).

181

182 **Alpha-6 integrins regulate the expression of laminin-511**

183 Since laminin-411 and laminin-511 have been associated with vessel maturation and
184 stability, we asked whether the loss of endothelial tube integrity after the depletion of α6
185 integrins was accompanied by changes in the expression of these laminins. We examined the
186 expression of the α5 and α4 laminin chains in planar co-culture assays in which we induced the
187 expression of either non-targeting or α6 targeting shRNAs after the formation of tubes as
188 described in Figure 3A. Our results indicate that the expression of the α5 chain of laminin-511 is
189 lost after the depletion of α6 integrins (Fig. 3C). In contrast, the LM α4 chain is still expressed,
190 but appears diffuse compared to control (Fig. 3C). The loss of laminin-511 may in part be due to
191 decreased levels of LM-α5 RNA (Fig. 4A). These results suggest that α6 integrins and laminin-
192 511 promote endothelial tube integrity.

193

194 **Laminin-511 and α6 integrins regulate the expression of the pro-angiogenic genes**
195 **CXCR4 and ANGPT2**

196 To gain further insight into the mechanisms by which endothelial laminins and α6 integrins
197 regulate tubular morphogenesis, we asked whether laminin-511 and α6 integrins regulate the
198 same set of angiogenesis-associated genes. Since depleting endothelial cells of laminin-411
199 also inhibited sprouting, we tested whether expression of the same or a distinct set of genes
200 was affected. We focused on the expression of genes previously associated with sprouting
201 angiogenesis. These include VEGFR2, CXCR4, ANGPT2, Dll4, PDGFB, NRP1, JAG1, and
202 MMP14 (De Smet et al., 2009; del Toro et al., 2010; Strasser et al., 2010). RNA was isolated
203 from non-targeting and α6 targeting shRNA expressing endothelial cells and gene expression
204 was analyzed by qPCR. Interestingly, depletion of either laminin-511 or α6 integrins led to
205 significant decreases in RNA transcripts for CXCR4 and ANGPT2 (Fig. 4A&C). Depleting
206 endothelial cells of laminin-411 had little effect on the expression of these genes (Fig. 4B).

207

208 **CXCR4 signaling is required for endothelial tubular morphogenesis**

209 Since the best characterized mechanism of action for angiopoietin-2, the product of the
210 ANGPT2 gene, is to antagonize the effects of angiopoietin-1 secreted by neighboring mural
211 cells (Carmeliet and Jain, 2011), we did not analyze the contribution of ANGPT2 expression in
212 our model. However, we did analyze the contribution of the chemokine receptor, CXCR4 to
213 endothelial morphogenesis in our organotypic models. CXCR4 has been previously implicated
214 in vascular development and angiogenesis (Salcedo and Oppenheim, 2003; Salvucci et al.,

215 2002; Tachibana et al., 1998; Unoki et al., 2010). Stromal-derived factor-1 (SDF-1) is a ligand
216 for CXCR4, and both endothelial cells (Salvucci et al., 2002) and fibroblasts (Nagasawa, 2014;
217 Quan et al., 2015) express SDF-1. Thus, it seemed possible that CXCR4 signaling is required
218 downstream of α6 integrins and laminin-511 for endothelial tubular morphogenesis. To test this
219 possibility, we used the pharmacological inhibitor AMD3100, which blocks CXCR4 activity
220 (Hatse et al., 2002 65; Kalatskaya et al., 2009). In dose response experiments, AMD3100
221 inhibited both the number and length of sprouts (Fig. 5A). Significant effects on sprout numbers
222 were observed at 500 nM, whereas sprout length was inhibited at concentrations as low as 100
223 nM (Fig. 5A). Similarly, endothelial morphogenesis was inhibited in planar co-culture assays in a
224 dose-dependent manner with significant inhibition starting at 100 nM of the inhibitor (Fig. 5B).
225 These data suggest that laminin-511 and α6 integrins regulate CXCR4 expression to promote
226 endothelial tubular morphogenesis.

227 **Discussion**

228 We used two organotypic co-culture models to demonstrate (1) that the endothelial
229 expression of laminin-411, laminin-511, and α6 integrins is required for tubular morphogenesis;
230 (2) that α6 integrins regulate the expression of laminin-511; (3) that laminin-511 and α6 integrins
231 regulate the expression of CXCR4 and ANGPT2; and (4) that CXCR4 signaling is a critical
232 component in the α6/laminin-511 morphogenesis response.

233 Several matrix proteins and integrin heterodimers can promote endothelial morphogenesis
234 and angiogenesis (Avraamides et al., 2008; Hynes, 2007; Senger and Davis, 2011). The
235 contribution of specific matrix proteins and integrins are context-dependent. Cell culture and
236 aortic ring explant cultures have been employed to examine the role of α6 integrins in tubular
237 morphogenesis and new vessel growth. Alpha-6 integrins were required when these assays
238 were performed in Matrigel, which is rich in laminin-111, a ligand for α6 integrins (Bouvard et al.,
239 2012; Primo et al., 2010). However, in collagen gels, α6 integrins were not required (Bouvard et
240 al., 2012; Primo et al., 2010). These findings suggest that the composition of the ECM
241 microenvironment can dictate usage of specific integrin heterodimers. However, endothelial
242 cells can secrete fibronectin, and endothelial expressed fibronectin and the αvβ3 and α5β1
243 fibronectin-binding integrins are essential for developmental retinal angiogenesis (Turner et al.,
244 2017). It is not clear why fibronectin expressed by endothelial cells does not override the
245 requirement for α6 integrins in assays performed in Matrigel. It is possible that the ECM
246 components present in the microenvironment together with the available angiogenic and other
247 growth factors dictate the role or regulate the expression of endothelial-secreted fibronectin,
248 suggesting that the contribution of endothelial fibronectin is context-dependent. This is
249 supported by the finding that endothelial expressed fibronectin and its integrin receptors are not
250 required for tumor angiogenesis (Murphy et al., 2015). Similarly, the reliance of α6 integrins and
251 endothelial-secreted laminin may also be context dependent. Both organotypic models present
252 an ECM microenvironment similar to that observed in wounds (Eming et al., 2007). In the planar
253 co-culture assay, there is a well-established fibronectin matrix secreted by fibroblasts, and the
254 bead sprout assay is performed in fibrin gels. The reliance of α6 integrins and endothelial-
255 secreted laminins could be due to a combination of the available matrix proteins and the growth
256 factor milieu present in these assays.

257 We analyzed the expression of a number of genes that are regulated during angiogenesis,
258 some of which are enriched in tips cells of sprouting vessels (De Smet et al., 2009; del Toro et
259 al., 2010; Strasser et al., 2010). The expression of the majority of genes interrogated did not
260 change upon depletion of either the LM-α5 chain or the integrin α6 subunit. However, the levels

261 of both CXCR4 and ANGPT2 were reduced upon the depletion of either α6 integrins or the LM-
262 α5 chain, suggesting that α6 integrins and LM-511 promotes their expression. Both the global
263 and endothelial specific knockout of CXCR4 resulted in defects in vascularization (Ara et al.,
264 2005). In our models, we demonstrated that tubular morphogenesis is regulated by CXCR4,
265 whose expression is regulated by α6 integrins and laminin-511. It is possible that CXCR4
266 signaling is a major regulator of endothelial morphogenesis in these models; thus, the
267 dependence on α6 integrins and laminin-511.
268 Our results also show that α6 integrins promote the expression of laminin-511 at least
269 partially through regulation of LM- α5 RNA. Furthermore, the loss of α6 integrins and the
270 concomitant loss of laminin-511 in established endothelial tubes resulted in the loss of their
271 structural integrity, suggesting that α6 integrins and laminin-511 contribute to vessel stability.
272 This is consistent with *in vivo* data discussed above demonstrating that the loss of expression of
273 α6 integrins in endothelial cells enhances tumor angiogenesis.
274 In contrast to the depletion of laminin-511, there was no overlap between the genes
275 regulated by loss of expression of the laminin-411 and the loss of α6 integrins. We anticipated
276 the down regulation of the Notch ligand, DLL4 upon LM-α4 depletion, as previous studies
277 demonstrated that DLL4 expression is down regulated in LM-α4 null mice during developmental
278 retinal angiogenesis (Stenzel et al., 2011). We also did not observe an obvious connection
279 between laminin-411 expression and the expression of α6 integrins, suggesting that another
280 integrin heterodimer engages laminin-411 to promote endothelial morphogenesis. The α2β1
281 integrin is a potential contributor as previous *in vitro* studies demonstrated that α2β1 plays a
282 central role in endothelial cell adhesion to laminin-411 (Stenzel et al., 2011).
283 In summary, the characterization of the contributions of laminins and α6 laminin-binding
284 integrins during angiogenesis in the adult is complicated by their roles in maintaining vessel
285 integrity (Miner et al., 1998; Thyboll et al., 2002; Turner et al., 2017). We were able to analyze
286 the role of endothelial-expressed laminins in early steps in tubular morphogenesis in the planar
287 co-culture and bead sprout assays, as endothelial morphogenesis in these models does not
288 require the disruption of established endothelial tubes. Our data support the conclusion that α6
289 integrins and laminin-511 positively regulates the expression of CXCR4 to promote early events
290 in tubular morphogenesis and also protects the integrity of established endothelial tubes.
291

292 **Materials and methods**

293 **Cell Culture**

294 Human umbilical vein endothelial cells (HUVECs) were from Lonza (Allendale, NJ) and were
295 cultured in in EGM-2 (Lonza, CC-3162). Adult human dermal fibroblasts (HDFs) were isolated
296 and characterized as previously described {Varney, 2016 #54; Zheng, 2019 #55) and
297 generously provided by the Van De Water laboratory (Albany Medical College). Human
298 embryonic kidney epithelial 293FT cells (HEK293FT) were a kind gift from Dr. Alejandro Pablo
299 Adam lab (AMC). HDFs and HEK293FT cells were cultured in DMEM (Sigma D6429) containing
300 10% FBS (Atlanta Biologicals), 100 units/ml penicillin (Life Technologies), 100 μg/ml
301 streptomycin (Life Technologies), and 2.92 μg/ml L-glutamine (GE LifeSciences). All cells were
302 cultured at 37°C in 5% CO2.
303

304 **Antibodies and Reagents**

305 Antibodies used in the study are from the following sources. Mouse monoclonal antibody to
306 CD31 (JC70A) was from Dako (Santa Clara, CA). Rabbit polyclonal antibody to CD31 (M-20)
307 was from Santa Cruz Biotechnology Inc. (Santa Cruz, CA). FITC-conjugated UEA lectin (L9006)
308 was from Sigma Aldrich (St. Louis, MO). Rat monoclonal to the α6 integrin subunit (GoH3) was
309 from BD Biosciences (Billerica, MA). Rabbit polyclonal antibody to Collagen IV (ab6586), rabbit
310 polyclonal antibody to laminin-111 (ab11575), mouse monoclonal antibody to the laminin α4
311 chain (ab205568), and mouse monoclonal antibody to the laminin α5 chain (ab77175) were
312 from Abcam (Cambridge, MA). Donkey anti-rat IgG Alexa Fluor 488 (A21208), donkey anti-
313 mouse IgG Alexa Fluor 488 (A21202), donkey anti-mouse IgG Alexa Fluor 568 (A10037), and
314 goat anti-rabbit IgG Alexa Fluor 488 (A11034) were from ThermoFisher Scientific (Waltham,
315 MA).
316

317 **siRNA**

318 HUVECs were plated in 6-well tissue culture plates and transfected with siRNA at a 50 nM
319 concentration with RNAiMAX (ThermoFisher) using the protocol provider by the manufacturer.
320 HUVECs transfected with siRNA were assayed for knockdown and used in planar co-cultures
321 (described below) 48 h after transfection. HUVECs transfected with siRNA and used in bead
322 sprout assays (described below) were transfected during bead coating and assayed for
323 knockdown at the end of experiment. siRNAs targeting were purchased from Sigma Aldrich (St.
324 Louis, MO). The non-targeting control was MISSION siRNA Universal Negative Control #1
325 (SIC001). The nucleotide sequences of targeting siRNAs are as follows: laminin α4 chain (5'-
326 GCAGAATCCTGCTATAGGA- 3'), laminin α5 chain (5'-CTGATCACCTGCACGGGCA-3'), and
327 the integrin α6 subunit (5'-GGATTGTTCGTGTAGAGCA-3').

328

329 **Inducible shRNA**

330 Doxycycline-inducible lentiviral (SMART) vectors harboring shRNAs targeting the α6 integrin
331 subunit or a non-targeting (NT) shRNA were purchased from Dharmacon (Lafayette, CO).
332 Lentiviruses were produced by co-transfection of HEK293FT cells with the shRNA expression
333 vector together with the packaging plasmid, psPAX2, coding for Gag, Pol, Rev, Tat (#12260,
334 Addgene), and the envelope plasmid, pMD2.G, coding for VSV-G (#12259, Addgene).
335 HUVECs were transduced with filtered viral supernatant plus 8 µg/ml polybrene. Cells were
336 induced with doxycycline (100 ng/ml) for 48 h prior to adding HUVECs to co-cultures or in some
337 experiments after 10 days in co-culture as described below. The nucleotide sequences of the
338 shRNAs are as follows: NT (5'-TGGTTTACATGTTGTGTGA-3'), α6 targeting sequence 1 (5'-
339 AAAACCACGGCTCCACTGT-3'), α6 targeting sequence 2 (5'-CTCCATGCACACTTTCTGT-3'),
340 and α6 targeting sequence 3 (5'-AACTCGATCCGCGTGCATG-3').

341

342 **Quantitative PCR (qPCR)**

343 TRIzol (ThermoFisher) was used to isolate RNA from siRNA transfected HUVECs, as well as,
344 shRNA expressing HUVECs. Extraction of RNA from bead sprout assays (described below)
345 using TRIzol was performed after the removal of HDFs with trypsin-EDTA Solution 10X (59418C,
346 Sigma). cDNA was synthesized with iScript Reverse Transcription Supermix (BioRad) using 1
347 µg of RNA. Equal amounts of cDNA were used in qPCR reactions performed with iQ SYBR
348 Green Supermix (BioRad). The nucleotide sequences of the qPCR primers used are listed in
349 Table 1.

350

351 **Western blotting**

352 Western blotting was used to confirm RNAi induced knockdown. Cells were lysed in mRIPA
353 buffer (50 mM Tris pH 7.4, 1% NP-40, 0.25% Na Deoxycholate, 150 mM NaCl, 1 mM EDTA)
354 containing both phosphatase (Sigma, #4906837001) and protease inhibitor cocktails
355 (ThermoFisher, 78440). Equal amounts of protein (20 to 40 µg) were separated by SDS-PAGE
356 and transferred to nitrocellulose for antibody probing. Imaging was performed with a ChemiDoc
357 XRS+ (BioRad) and quantitation with Image Lab (BioRad).

358

359 **Organotypic culture assays**

360 <u>Planar co-culture</u>: As one organotypic culture, we utilized the planar co-culture model developed
361 by Bishop and colleagues (Bishop et al., 1999) and modified by the Pumiglia lab (Bajaj et al.,

362 2012). This model reconstitutes some of the complex interactions that occur during
363 angiogenesis among endothelial cells, the ECM and supporting cells. HDFs were seeded in
364 tissue cultures dishes ± glass coverslips and cultured to confluence. The medium was changed
365 to EGM-2. HUVECs, expressing targeting or non-targeting RNAi, were then seeded 16 h later at
366 a density of 20,000 cells per 9 cm^2 and cultured up to 10 days. ShRNA-mediated knockdown in
367 pre-formed tubes was accomplished by culturing HUVECs expressing doxycycline-inducible
368 lentiviral (SMART) vectors on HDFs for 10 days, in the absence of doxycycline with medium
369 changed every 48 h. Doxycycline was then introduced on day 11, at a concentration of 100
370 ng/ml and refreshed every 48 h for up to 16 days. Endothelial morphogenesis and changes in
371 tube structure were analyzed by immunofluorescence microscopy.
372
373 Bead sprout assay: To study endothelial sprouting, we employed the bead sprout assay as
374 described by Nakatsu and Hughes (Nakatsu and Hughes, 2008). Cytodex 3 beads (GE) were
375 coated at ~1000 HUVECs per bead inside of a 2 ml microcentrifuge tube for 4 at 37°C, mixing
376 gently by inverting the tubes every 20 min and transferred to a T25 flask and incubated at 37°C,
377 overnight. Beads were then washed 3X with EGM-2 medium and re-suspended in PBS
378 containing 3 mg/ml of fibrinogen (Sigma, #F8630) and 0.15 U/ml of aprotinin (Sigma, #A6279).
379 Thrombin (Sigma, #T4648) was added at a final concentration of 0.125 U/ml and the mixture
380 was plated in wells of and 8-well slide (Corning, #3-35411). The mixture was allowed to clot for
381 30 min at 37°C. HDFs were then added to the top surface of the fibrin gel in EGM-2 medium at
382 a concentration of 30,000 cells per well. The formation of sprouts and sprout lengths were
383 assayed by either immunofluorescence of phase contrast microscopy.
384
385 **Immunofluorescence Microscopy**
386 Cells were fixed cells with 4% PFA (Electron Microscopy Sciences) for 15 min, permeabilized
387 with 0.5% Triton X-100 in PBS for 15 min, and then blocked with 2% BSA in PBST for 1 h at RT.
388 Antibodies were diluted in 2% BSA in PBST and incubated with cells overnight at 4°C. Samples
389 were then washed 4X with PBST at RT over the course of 4 h, and then incubated for 1 h with
390 the appropriate secondary antibodies (1:1000 dilution). Following secondary antibody staining,
391 samples were washed 3X with PBST at RT for 1 h and mounted with SlowFade Gold antifade
392 reagent (ThermoFisher). Samples were analyzed using a Nikon inverted TE2000-E microscope
393 equipped with phase contrast and epifluorescence, a digital CoolSNAP HQ camera, a Prior
394 ProScanII motorized stage and a Nikon C1 confocal system and EZC1 and NIS-Elements
395 acquisition software. Images were acquired with Plan Fluor 4X/0.13, Plan Fluor 10X/0.30, Plan

Fluor ELWD 20X/0.45, Plan Apo 40X/1.0 oil, and Plan Apo 100X/1.4 oil objectives and analyzed with either NIS elements (Nikon) or IMARIS software as indicated. Contrast and/or brightness were adjusted for some images to assist in visualization.

Image analysis

For planar co-cultures, were endothelial cells initially form cell trains/cord, which mature into endothelial tubes, cord/tube lengths in planar co-cultures were measured by tracing tubes within each field using NIS Elements (Nikon). Any tubes that extend beyond the field were excluded from analysis. Tube widths in planar co-cultures were calculated with AngioTool (NIH) by dividing total tube area by total tube lengths per field. Sprout lengths in bead sprout assays were measured by tracing each sprout using NIS elements (Nikon) and sprouts per bead were counted manually.

Statistical analysis

Statistical analysis was performed with GraphPad Prism software using Student's t-test or one-way ANOVA. P value of $p<0.05$ was considered to be statistically significant.

Acknowledgements

The authors thank Drs. Livingston Van De Water and C Michael DiPersio for critically reading this manuscript, Dr. Van De Water for providing human adult dermal fibroblasts, and Debbie Moran for assistance in the preparation of the figures.

Competing interests

No competing interests declared.

Funding

This work was supported by Institutional seed funds to SEL and by funding from the David E Bryant Foundation to KP

Data availability

All reagents generated in this study will be made available upon request.

429 **References**

430

431 Ara, T., K. Tokoyoda, R. Okamoto, P.A. Koni, and T. Nagasawa. 2005. The role of CXCL12 in
432 the organ-specific process of artery formation. *Blood*. 105:3155-3161.
433 Avraamides, C.J., B. Garmy-Susini, and J.A. Varner. 2008. Integrins in angiogenesis and
434 lymphangiogenesis. *Nat Rev Cancer*. 8:604-617.
435 Bajaj, A., Q.F. Li, Q. Zheng, and K. Pumiglia. 2012. Loss of NF1 expression in human
436 endothelial cells promotes autonomous proliferation and altered vascular morphogenesis.
437 *PLoS One*. 7:e49222.
438 Bishop, E.T., G.T. Bell, S. Bloor, I.J. Broom, N.F. Hendry, and D.N. Wheatley. 1999. An in vitro
439 model of angiogenesis: basic features. *Angiogenesis*. 3:335-344.
440 Bouvard, C., A. De Arcangelis, B. Dizier, I. Galy-Fauroux, A.M. Fischer, E. Georges-Labouesse,
441 and D. Helley. 2012. Tie2-dependent knockout of alpha6 integrin subunit in mice
442 reduces post-ischaemic angiogenesis. *Cardiovasc Res*. 95:39-47.
443 Bouvard, C., B. Gafsou, B. Dizier, I. Galy-Fauroux, A. Lokajczyk, C. Boisson-Vidal, A.M. Fischer,
444 and D. Helley. 2010. alpha6-integrin subunit plays a major role in the proangiogenic
445 properties of endothelial progenitor cells. *Arterioscler Thromb Vasc Biol*. 30:1569-1575.
446 Bouvard, C., Z. Segaoula, A. De Arcangelis, I. Galy-Fauroux, L. Mauge, A.M. Fischer, E.
447 Georges-Labouesse, and D. Helley. 2014. Tie2-dependent deletion of alpha6 integrin
448 subunit in mice reduces tumor growth and angiogenesis. *Int J Oncol*. 45:2058-2064.
449 Carmeliet, P. 2003. Angiogenesis in health and disease. *Nat Med*. 9:653-660.
450 Carmeliet, P. 2005. Angiogenesis in life, disease and medicine. *Nature*. 438:932-936.
451 Carmeliet, P., and R.K. Jain. 2011. Molecular mechanisms and clinical applications of
452 angiogenesis. *Nature*. 473:298-307.
453 Danen, E.H., and A. Sonnenberg. 2003. Integrins in regulation of tissue development and
454 function. *J Pathol*. 201:632-641.
455 Davis, G.E., and D.R. Senger. 2005. Endothelial extracellular matrix: biosynthesis, remodeling,
456 and functions during vascular morphogenesis and neovessel stabilization. *Circ Res*.
457 97:1093-1107.
458 De Smet, F., I. Segura, K. De Bock, P.J. Hohensinner, and P. Carmeliet. 2009. Mechanisms of
459 vessel branching: filopodia on endothelial tip cells lead the way. *Arterioscler Thromb*
460 *Vasc Biol*. 29:639-649.

461 del Toro, R., C. Prahst, T. Mathivet, G. Siegfried, J.S. Kaminker, B. Larrivee, C. Breant, A.
462 Duarte, N. Takakura, A. Fukamizu, J. Penninger, and A. Eichmann. 2010. Identification
463 and functional analysis of endothelial tip cell-enriched genes. *Blood*. 116:4025-4033.
464 Eming, S.A., B. Brachvogel, T. Odorisio, and M. Koch. 2007. Regulation of angiogenesis:
465 wound healing as a model. *Prog Histochem Cytochem*. 42:115-170.
466 Germain, M., A. De Arcangelis, S.D. Robinson, M. Baker, B. Tavora, G. D'Amico, R. Silva, V.
467 Kostourou, L.E. Reynolds, A. Watson, J.L. Jones, E. Georges-Labouesse, and K.
468 Hodivala-Dilke. 2010. Genetic ablation of the alpha 6-integrin subunit in Tie1Cre mice
469 enhances tumour angiogenesis. *J Pathol*. 220:370-381.
470 Hallmann, R., N. Horn, M. Selg, O. Wendler, F. Pausch, and L.M. Sorokin. 2005. Expression
471 and function of laminins in the embryonic and mature vasculature. *Physiol Rev*. 85:979-
472 1000.
473 Hatse, S., K. Princen, G. Bridger, E. De Clercq, and D. Schols. 2002. Chemokine receptor
474 inhibition by AMD3100 is strictly confined to CXCR4. *FEBS Lett*. 527:255-262.
475 Hynes, R.O. 2007. Cell-matrix adhesion in vascular development. *J Thromb Haemost*. 5 Suppl
476 1:32-40.
477 Kalatskaya, I., Y.A. Berchiche, S. Gravel, B.J. Limberg, J.S. Rosenbaum, and N. Heveker. 2009.
478 AMD3100 is a CXCR7 ligand with allosteric agonist properties. *Mol Pharmacol*. 75:1240-
479 1247.
480 Kortesmaa, J., P. Yurchenco, and K. Tryggvason. 2000. Recombinant laminin-8
481 (alpha(4)beta(1)gamma(1)). Production, purification,and interactions with integrins. *J Biol*
482 *Chem*. 275:14853-14859.
483 Lee, T.H., S. Seng, H. Li, S.J. Kennel, H.K. Avraham, and S. Avraham. 2006. Integrin regulation
484 by vascular endothelial growth factor in human brain microvascular endothelial cells: role
485 of alpha6beta1 integrin in angiogenesis. *J Biol Chem*. 281:40450-40460.
486 Mavria, G., Y. Vercoulen, M. Yeo, H. Paterson, M. Karasarides, R. Marais, D. Bird, and C.J.
487 Marshall. 2006. ERK-MAPK signaling opposes Rho-kinase to promote endothelial cell
488 survival and sprouting during angiogenesis. *Cancer Cell*. 9:33-44.
489 Miner, J.H., J. Cunningham, and J.R. Sanes. 1998. Roles for laminin in embryogenesis:
490 exencephaly, syndactyly, and placentopathy in mice lacking the laminin alpha5 chain. *J*
491 *Cell Biol*. 143:1713-1723.
492 Murphy, P.A., S. Begum, and R.O. Hynes. 2015. Tumor angiogenesis in the absence of
493 fibronectin or its cognate integrin receptors. *PLoS One*. 10:e0120872.

494 Nagasawa, T. 2014. CXC chemokine ligand 12 (CXCL12) and its receptor CXCR4. *J Mol Med*
495 *(Berl)*. 92:433-439.
496 Nakatsu, M.N., and C.C. Hughes. 2008. An optimized three-dimensional in vitro model for the
497 analysis of angiogenesis. *Methods Enzymol*. 443:65-82.
498 Nakatsu, M.N., R.C. Sainson, J.N. Aoto, K.L. Taylor, M. Aitkenhead, S. Perez-del-Pulgar, P.M.
499 Carpenter, and C.C. Hughes. 2003. Angiogenic sprouting and capillary lumen formation
500 modeled by human umbilical vein endothelial cells (HUVEC) in fibrin gels: the role of
501 fibroblasts and Angiopoietin-1. *Microvasc Res*. 66:102-112.
502 Primo, L., G. Seano, C. Roca, F. Maione, P.A. Gagliardi, R. Sessa, M. Martinelli, E. Giraudo, L.
503 di Blasio, and F. Bussolino. 2010. Increased expression of alpha6 integrin in endothelial
504 cells unveils a proangiogenic role for basement membrane. *Cancer Res*. 70:5759-5769.
505 Quan, C., M.K. Cho, Y. Shao, L.E. Mianecki, E. Liao, D. Perry, and T. Quan. 2015. Dermal
506 fibroblast expression of stromal cell-derived factor-1 (SDF-1) promotes epidermal
507 keratinocyte proliferation in normal and diseased skin. *Protein Cell*. 6:890-903.
508 Salcedo, R., and J.J. Oppenheim. 2003. Role of chemokines in angiogenesis: CXCL12/SDF-1
509 and CXCR4 interaction, a key regulator of endothelial cell responses. *Microcirculation*.
510 10:359-370.
511 Salvucci, O., L. Yao, S. Villalba, A. Sajewicz, S. Pittaluga, and G. Tosato. 2002. Regulation of
512 endothelial cell branching morphogenesis by endogenous chemokine stromal-derived
513 factor-1. *Blood*. 99:2703-2711.
514 Samarelli, A.V., E. Riccitelli, L. Bizzozero, T.N. Silveira, G. Seano, M. Pergolizzi, G. Vitagliano, I.
515 Cascone, G. Carpentier, A. Bottos, L. Primo, F. Bussolino, and M. Arese. 2014.
516 Neuroligin 1 induces blood vessel maturation by cooperating with the alpha6 integrin. *J*
517 *Biol Chem*. 289:19466-19476.
518 Senger, D.R., and G.E. Davis. 2011. Angiogenesis. *Cold Spring Harb Perspect Biol*. 3:a005090.
519 Song, J., X. Zhang, K. Buscher, Y. Wang, H. Wang, J. Di Russo, L. Li, S. Lutke-Enking, A.
520 Zarbock, A. Stadtmann, P. Striewski, B. Wirth, I. Kuzmanov, H. Wiendl, D. Schulte, D.
521 Vestweber, and L. Sorokin. 2017. Endothelial Basement Membrane Laminin 511
522 Contributes to Endothelial Junctional Tightness and Thereby Inhibits Leukocyte
523 Transmigration. *Cell Rep*. 18:1256-1269.
524 Stenzel, D., C.A. Franco, S. Estrach, A. Mettouchi, D. Sauvaget, I. Rosewell, A. Schertel, H.
525 Armer, A. Domogatskaya, S. Rodin, K. Tryggvason, L. Collinson, L. Sorokin, and H.
526 Gerhardt. 2011. Endothelial basement membrane limits tip cell formation by inducing
527 Dll4/Notch signalling in vivo. *EMBO Rep*. 12:1135-1143.

528 Strasser, G.A., J.S. Kaminker, and M. Tessier-Lavigne. 2010. Microarray analysis of retinal
529 endothelial tip cells identifies CXCR4 as a mediator of tip cell morphology and branching.
530 *Blood*. 115:5102-5110.
531 Streuli, C.H., and N. Akhtar. 2009. Signal co-operation between integrins and other receptor
532 systems. *Biochem J*. 418:491-506.
533 Tachibana, K., S. Hirota, H. Iizasa, H. Yoshida, K. Kawabata, Y. Kataoka, Y. Kitamura, K.
534 Matsushima, N. Yoshida, S. Nishikawa, T. Kishimoto, and T. Nagasawa. 1998. The
535 chemokine receptor CXCR4 is essential for vascularization of the gastrointestinal tract.
536 *Nature*. 393:591-594.
537 Thyboll, J., J. Kortesmaa, R. Cao, R. Soininen, L. Wang, A. Iivanainen, L. Sorokin, M. Risling, Y.
538 Cao, and K. Tryggvason. 2002. Deletion of the laminin alpha4 chain leads to impaired
539 microvessel maturation. *Mol Cell Biol*. 22:1194-1202.
540 Turner, C.J., K. Badu-Nkansah, and R.O. Hynes. 2017. Endothelium-derived fibronectin
541 regulates neonatal vascular morphogenesis in an autocrine fashion. *Angiogenesis*.
542 20:519-531.
543 Unoki, N., T. Murakami, K. Nishijima, K. Ogino, N. van Rooijen, and N. Yoshimura. 2010. SDF-
544 1/CXCR4 contributes to the activation of tip cells and microglia in retinal angiogenesis.
545 *Invest Ophthalmol Vis Sci*. 51:3362-3371.
546 Yurchenco, P.D. 2011. Basement membranes: cell scaffoldings and signaling platforms. *Cold*
547 *Spring Harb Perspect Biol*. 3.
548
549

550 **Figure Legends**

551

552 **Figure 1. Laminin-411 and laminin-511 regulate endothelial tubular morphogenesis**
553 **(A-B)** Endothelial basement membrane components are expressed in co-culture.
554 Immunofluorescence staining of 3-day planar co-cultures **(A)** or 6-day bead sprouts **(B)** shows
555 endothelial expression of the laminin α4 (LM-α4) and α5 (LM-α5) chains, the laminin (LM) β1
556 and γ1 chains, as well as COL IV. Scale bar = 50 μm and 100 μm respectively. **(C-I)** Depletion
557 of either the LM-α4 or LM-α5 chain inhibits endothelial morphogenesis. **(C-D)** The efficiency of
558 siRNA-mediated knockdown of the LM-α4 chain **(C)** and LM-α5 chain **(D)** in endothelial cells
559 used in functional studies was assayed by qPCR for each of the three independent experiments
560 and plotted as the mean ± s.d. **(E)** Representative images of RFP-expressing endothelial cells
561 at day 2 of planar co-culture depleted of either the LM-α4 or LM-α5 chain compared to control.
562 Scale = 100 μm. **(F)** Quantitation of endothelial cord length at day 2 for the different conditions.
563 Plotted is length of endothelial cords measured from 10 random fields in 3 independent
564 experiments. Data was analyzed by one-way ANOVA and plotted as the mean length ± s.d. **(G)**
565 Representative images of endothelial cells depleted of either the Lm α4 or α5 chain in a 5-day
566 bead sprout assay showing decreased sprout length and sprouts number per bead compared to
567 control. Arrows indicate examples of sprouts. Scale = 250 μm. **(H-I)** Quantitation of number of
568 sprouts **(H)** or sprout length **(I)** from 6-8 beads in each of 10 randomly selected fields in 3
569 independent experiments. Plotted are the **(H)** number of sprouts on individual beads or **(I)** or the
570 length of individual sprouts **(I)**. Data was analyzed by one-way ANOVA. The mean ± s.d. is
571 indicated.

572

573 **Figure 2. Depletion of endothelial α6 integrins inhibits endothelial tubulogenesis. (A)**
574 Immunofluorescence staining of 2-day planar co-cultures indicating the endothelial expression
575 of α6 integrins. **(B)** Alpha-6 integrins were depleted in endothelial cells by shRNA and the
576 effects were assayed in 3 independent experiments. Efficiency of knockdown was assayed by
577 western blot (left panel) Statistical analysis was performed with a two-tailed Student's t-test. The
578 mean ± s.d is indicated. The effect of α6 depletion on cord/tube length in planar co-culture was
579 assayed every 2 days for 10 days and compared to control. Cord/tube length was quantified in
580 three independent experiments. Plotted with the length of individual cords/tubes with each
581 experiment represent by a different color (middle panel). Representative images are shown from
582 the 6-day co-cultures (right panel). Scale = 100 μm. **(C)** Similar effects of α6 knockdown were
583 observed in bead sprout assays (left panel). Efficiency of α6 knockdown was determined by

584 western blot. Statistical analysis was performed using a two-tailed Student's t-test. The mean ±
585 s.d. is indicated (left panel). Sprout length was measured every 2 days for 8 days. Plotted is the
586 length of individual sprouts from 3 independent experiments with each experiment represented
587 by a different color. Representative images of 8-day bead sprouts assays are shown in the Left
588 Panel. Scale = 500 μm. *p ≤ 0.05, **p ≤ 0.01.
589
590 **Figure 3. Depletion of α6 integrins from established endothelial tubes disrupts tube**
591 **integrity and inhibits the expression of laminin-511. (A-B)** Depleting endothelial tubes of α6
592 integrins inhibits tube stability. Endothelial tubes were formed for 10 days in the planar co-
593 culture assay and the expression of α6 or non-targeting shRNA was induced with doxycycline.
594 **(A)** Representative images of endothelial tubes after 8 and 12 days of induction of either the α6
595 or non-targeting (NT) shRNA. **(B)** The disruption of endothelial tubes resulted in altered
596 morphology best characterized by an increase in the width of the resulting endothelial structures.
597 Plotted is the average width of individual tubes/field (NT-shRNA) and endothelial structures (α6-
598 shRNA) measured from ten randomly selected fields in two independent experiments. n=22.
599 Student's t was used to compare conditions. The mean ± s.d. is indicated. ***p ≤ 0.001. **(C)**
600 Comparison of laminin-411 and laminin-511 in endothelial tubes after the depletion of α6
601 integrins. The depletion of α6 integrins from stable endothelial tubes was performed as
602 described above. Both endothelial laminins are expressed by stable endothelial tubes as shown
603 in the NT control. Depletion of α6 resulted in the loss of laminin-511, but not laminin-411. Scale
604 = 50 μm.
605
606 **Figure 4. The expression of the CXCR4 and ANGPT2 genes are positively regulated by α6**
607 **integrins and laminin-511. (A-B)** RNA was isolated from 6-day bead sprouts and analyzed by
608 qPCR. **(A**) Shown is the efficiency of α6 depletion and the effects of α6 depletion on the
609 expression of the LM-α4, LM- α5, CXCR4 and ANGPT2 normalized to non-targeting control. **(B)**
610 Shown is the efficiency of depletion of the LM-α4 chain and the effects of this depletion of the
611 expression of CXCR4 and ANGPT2. **(C)** Shown is the efficiency of depletion of the LM-α5 chain
612 and the effects of this depletion of the expression of CXCR4 and ANGPT2. n = 3, **p ≤ 0.01,
613 ***p ≤ 0.001, ****p ≤ 0.0001.
614
615 **Figure 5. Pharmacological inhibition of the CXCR4 receptor inhibits endothelial tubular**
616 **morphogenesis organotypic culture. (A)** The dose-dependent reduction in the number of
617 endothelial sprouts, as well as sprout length in 6-day bead sprout assays in response to the

618 CXCR4 inhibitor, AMD3100. Left panel - Plotted is the number of sprouts on individual beads
619 from 3 fields containing 7-10 beads from each of two independent experiments. The mean and
620 s.d. are indicated. Right panel- Plotted is the length of individual sprouts on these same beads
621 **(B)** AMD3100 inhibition of CXCR4 in 6-day planar co-culture causes defective morphogenesis
622 in a dose-dependent manner. Representative images are shown in the Right Panel. Scale = 100
623 μm. Left Panel- Plotted is the average length of cords/tubes fields. Six fields were analyzed in
624 each of two independent experiments. The mean ± s.d. is indicated. One-way ANOVA was used
625 to compare sprouts or tube lengths. **$p \leq 0.01$, ***$p \leq 0.001$ ****$p \leq 0.0001$.
626
627
628
629
630

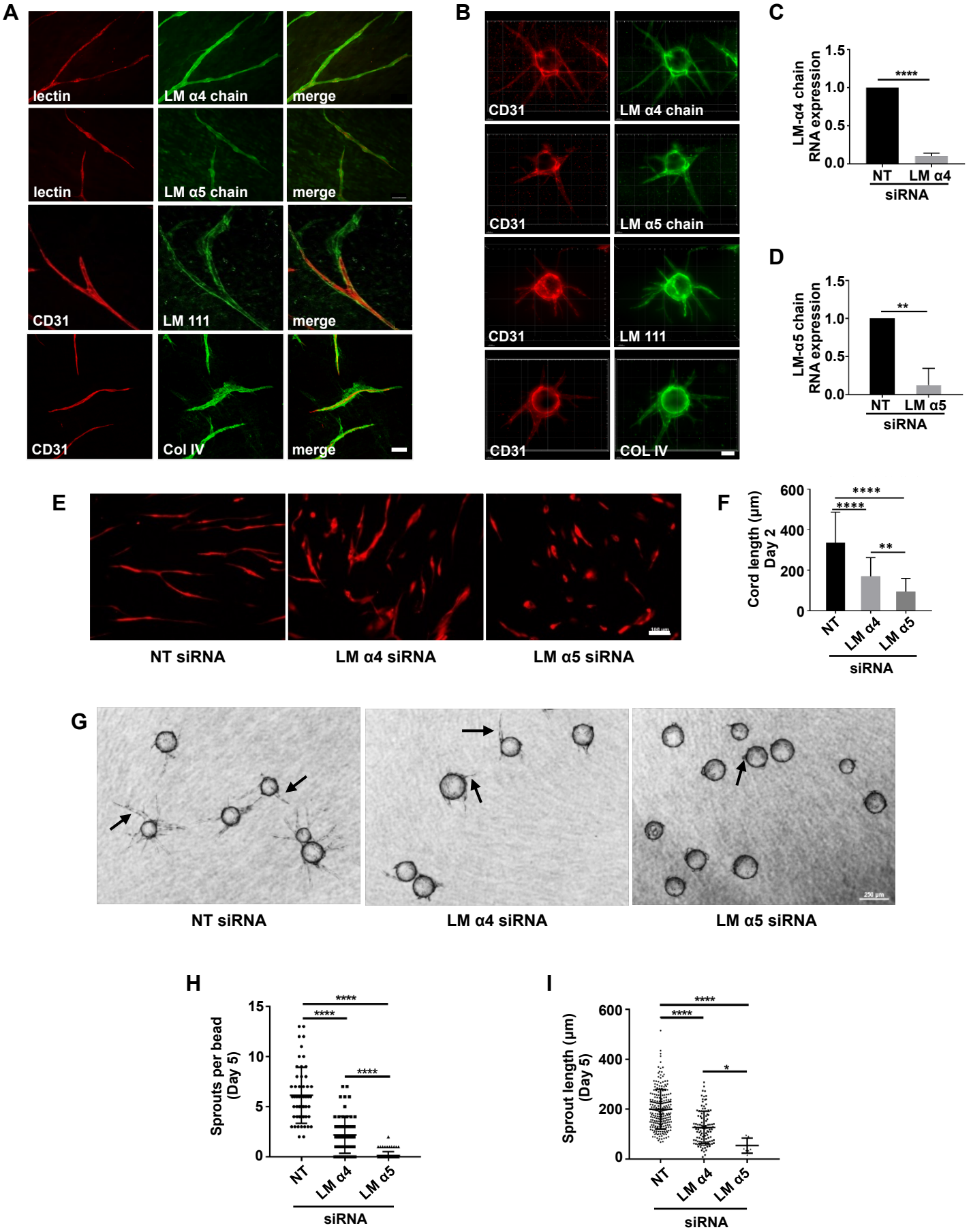
A
lectin
LM α4 chain
merge
lectin
LM α5 chain
merge
CD31
LM 111
merge
CD31
Col IV
merge
B
CD31
LM α4 chain
CD31
LM α5 chain
CD31
LM 111
CD31
COL IV
C
LM-α4 chain RNA expression
1.5
1.0
0.5
0.0
****
NT
LM α4
siRNA
D
LM-α5 chain RNA expression
1.5
1.0
0.5
0.0
**
NT
LM α5
siRNA
E
NT siRNA
LM α4 siRNA
LM α5 siRNA
F
Cord length (µm) Day 2
600
400
200
0
****
****
**
NT
LM α4
LM α5
siRNA
G
NT siRNA
LM α4 siRNA
LM α5 siRNA
H
Sprouts per bead (Day 5)
15
10
5
0
****
****
****
NT
LM α4
LM α5
siRNA
I
Sprout length (µm) (Day 5)
600
400
200
0
****
****
*
NT
LM α4
LM α5
siRNA

Figure 1

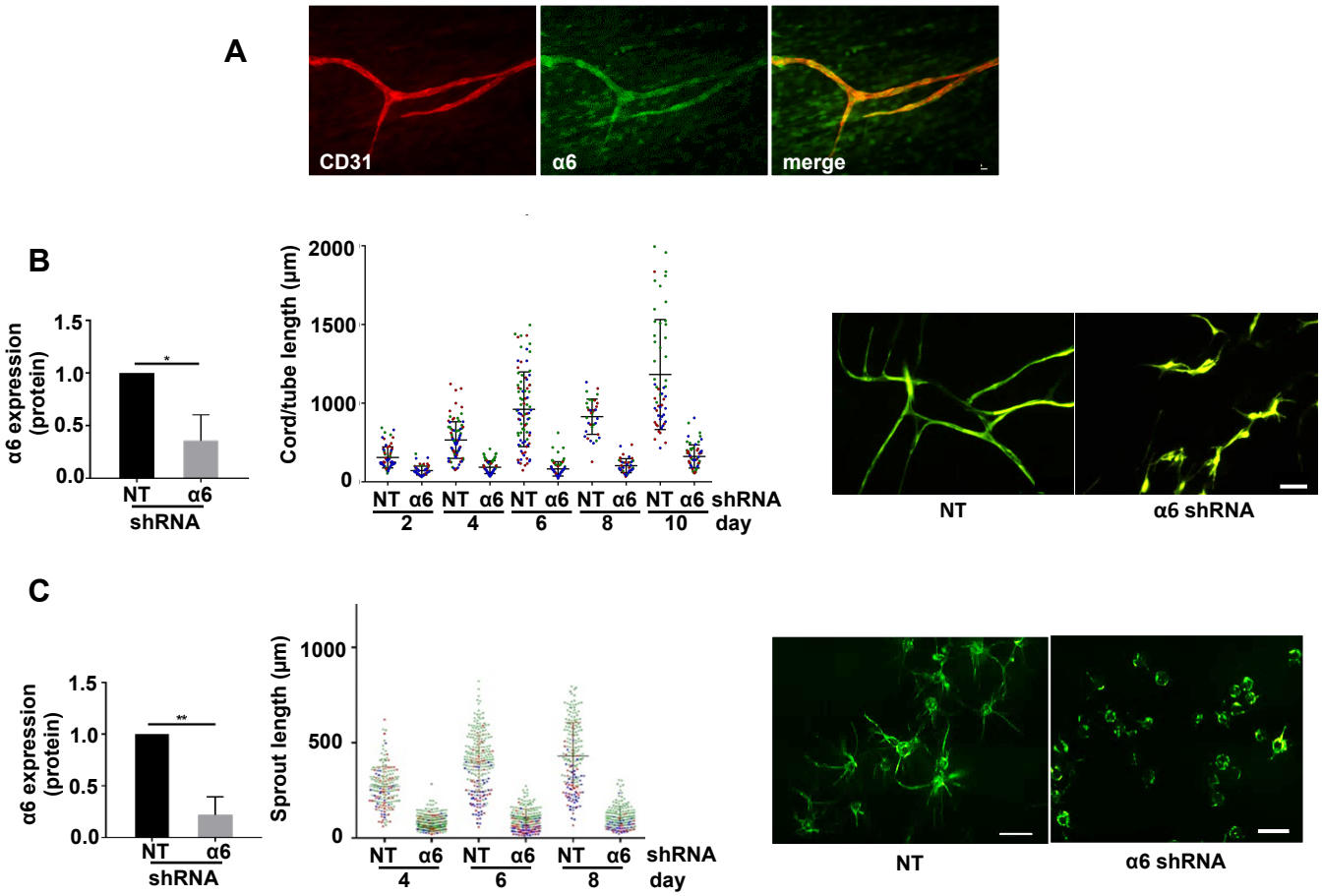
A
CD31
α6
merge
B
α6 expression (protein)
1.5
1.0
0.5
0.0
*
NT
α6
shRNA
Cord/tube length (μm)
2000
1500
1000
0
NT α6 NT α6 NT α6 NT α6 NT α6 shRNA
2 4 6 8 10 day
NT
α6 shRNA
C
α6 expression (protein)
1.5
1.0
0.5
0.0
**
NT
α6
shRNA
Sprout length (μm)
1000
500
0
NT α6 NT α6 NT α6 shRNA
4 6 8 day
NT
α6 shRNA

Figure 2

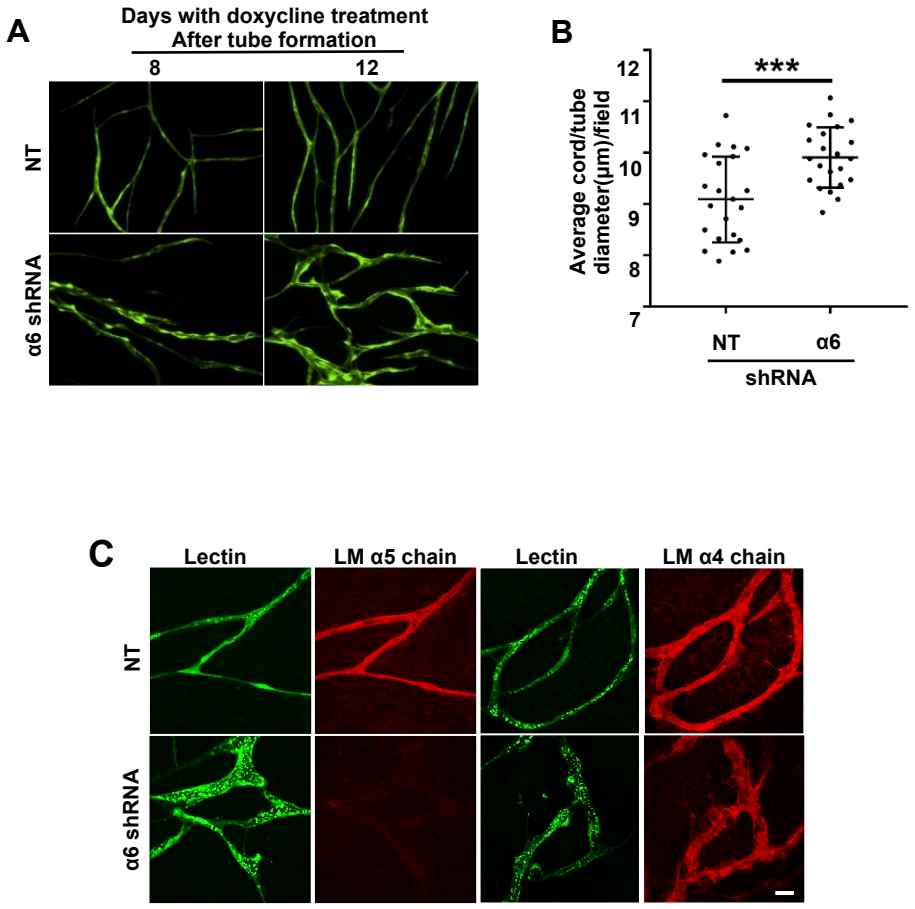
A
Days with doxycline treatment
After tube formation
8
12
NT
α6 shRNA
B
***
Average cord/tube diameter(μm)/field
12
11
10
9
8
7
NT
α6
shRNA
C
Lectin
LM α5 chain
Lectin
LM α4 chain
NT
α6 shRNA

Figure 3

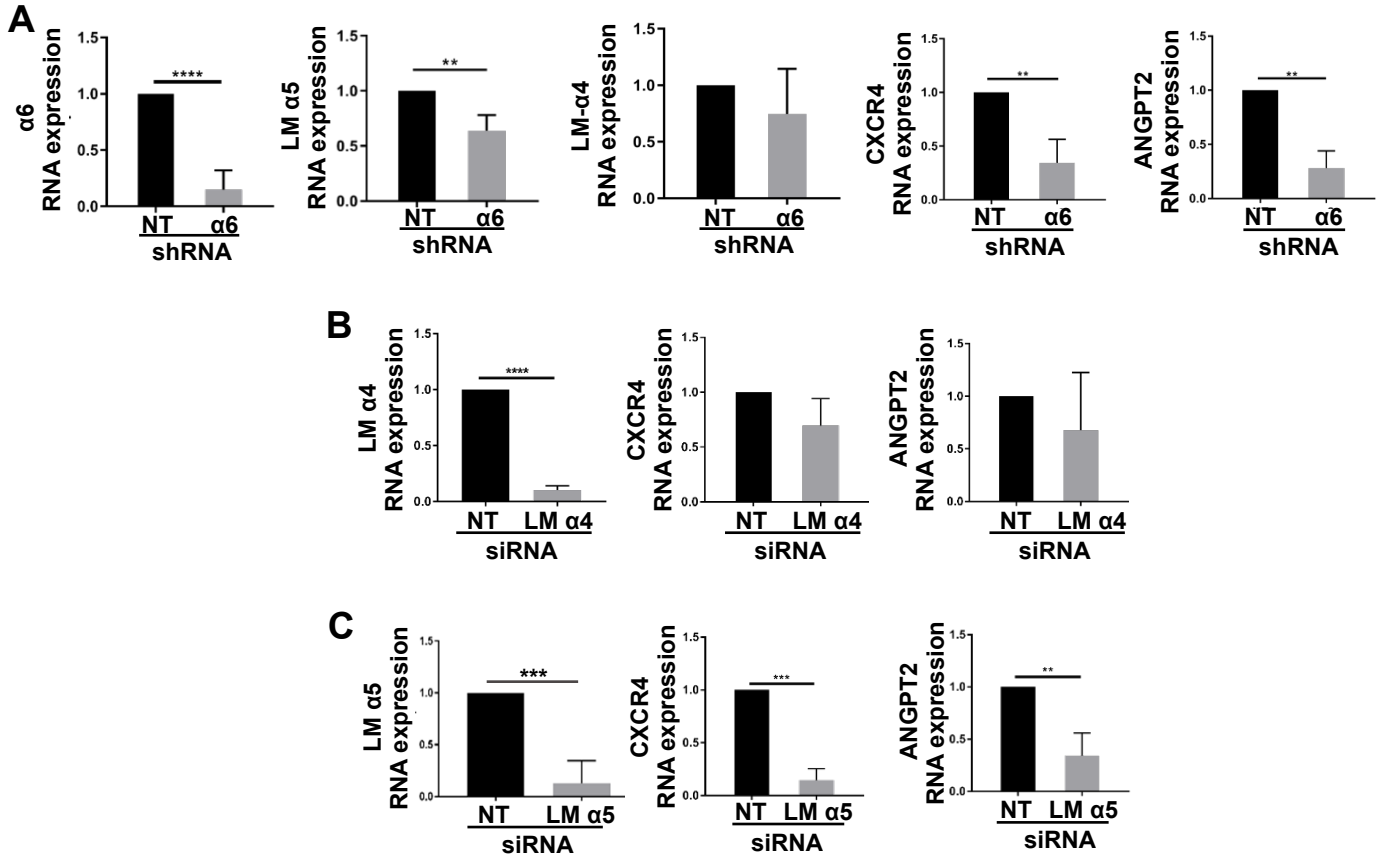
A
α6 RNA expression
****
NT α6
shRNA
LM α5 RNA expression
**
NT α6
shRNA
LM-α4 RNA expression
NT α6
shRNA
CXCR4 RNA expression
**
NT α6
shRNA
ANGPT2 RNA expression
**
NT α6
shRNA
B
LM α4 RNA expression
****
NT LM α4
siRNA
CXCR4 RNA expression
NT LM α4
siRNA
ANGPT2 RNA expression
NT LM α4
siRNA
C
LM α5 RNA expression
***
NT LM α5
siRNA
CXCR4 RNA expression
***
NT LM α5
siRNA
ANGPT2 RNA expression
**
NT LM α5
siRNA

Figure 4

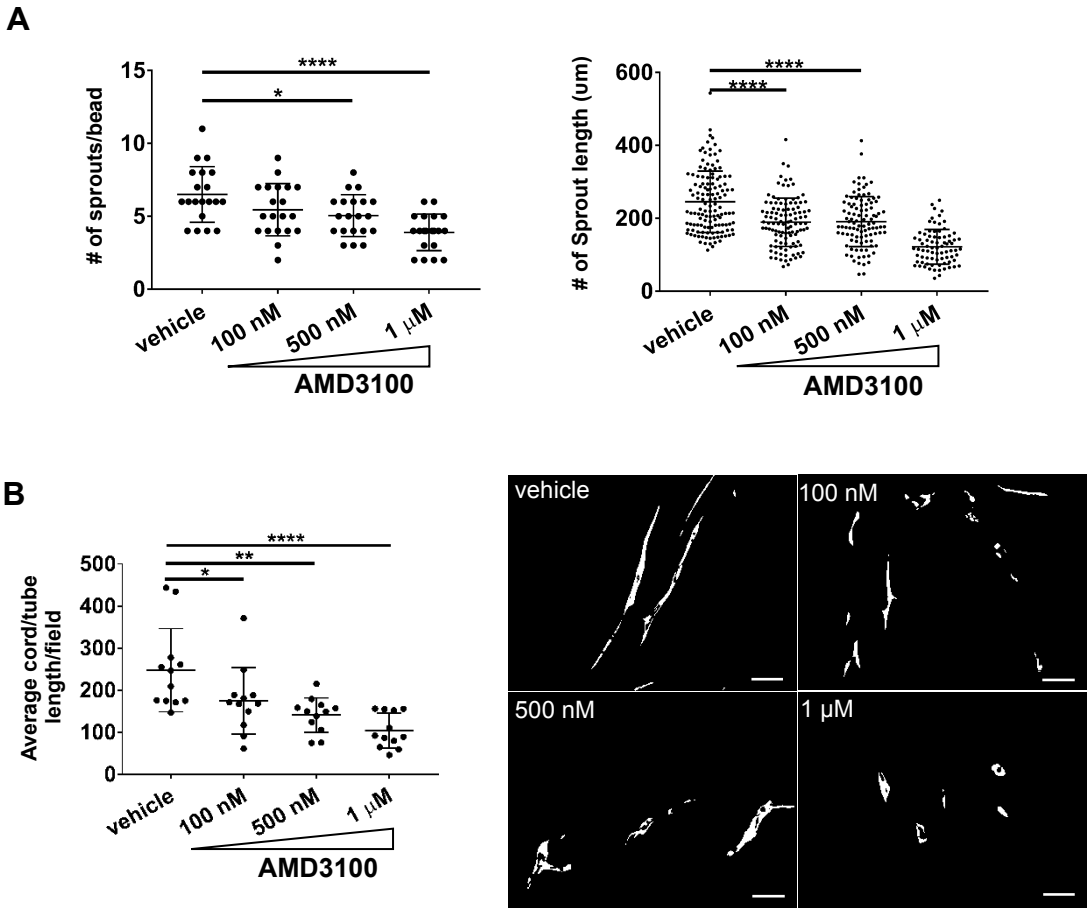
A
# of sprouts/bead
15
10
5
0
****
*
vehicle
100 nM
500 nM
1 μM
AMD3100
# of Sprout length (um)
600
400
200
0
****
****
vehicle
100 nM
500 nM
1 μM
AMD3100
B
Average cord/tube length/field
500
400
300
200
100
0
****
**
*
vehicle
100 nM
500 nM
1 μM
AMD3100
vehicle
100 nM
500 nM
1 μM

Figure 5

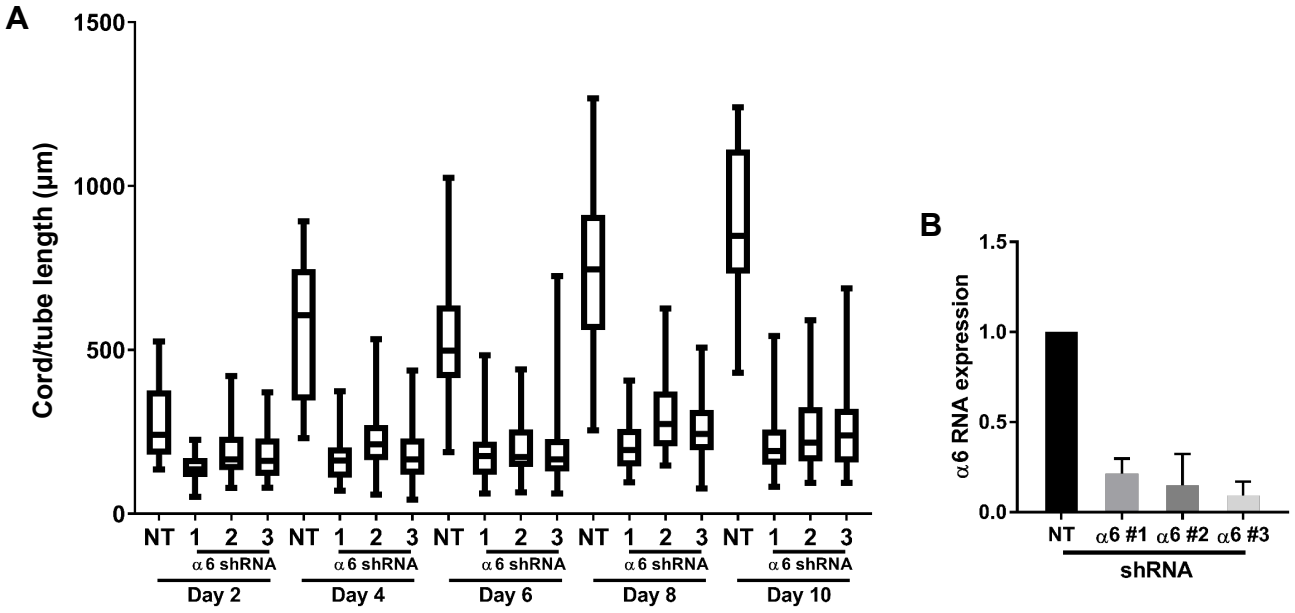

Supplemental Figure 1. (A) Depletion of endothelial α6 integrins using 3 independent shRNA targeting sequences shows similar inhibition of tubular morphogenesis compared to control. Cord/ tube lengths were collected from 10 randomly selected fields in 3 independent experiments. **(B)** Knockdown of α6 was confirmed using qPCR. Mean RNA expression is from 3 independent experiments. Alpha 6 targeting sequence 2 was used in Figures 2, 3, and 4 of main text.

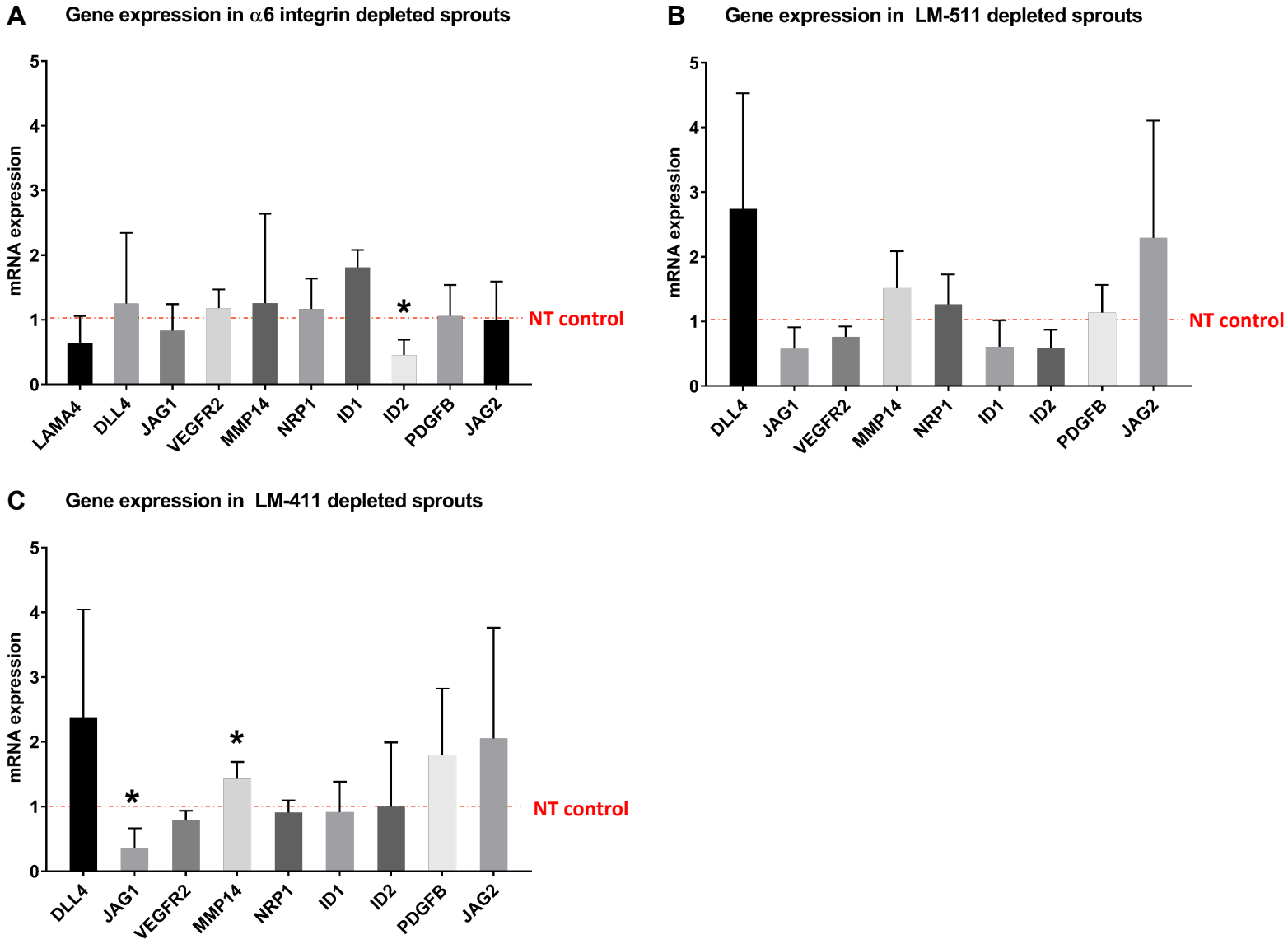

Supplemental Figure 2. Expression of angiogenesis-associated genes in 5-day bead sprout assay compared to control **(A)** alpha 6 integrin-depleted endothelial cells **(B)** laminin-511-depleted endothelial cells and **(C)** laminin-411-depleted endothelial cells were measured by qPCR. Data are plotted as the mean ± s.d. from 3 independent experiments. Expression of each gene was compared to NT control using two-way Student's T-test. *$p \leq 0.05$.